

IDENTIFYING AND TUNING SAFETY NEURONS IN LARGE LANGUAGE MODELS

Anonymous authors

Paper under double-blind review

ABSTRACT

Safety alignment for Large Language Models (LLMs) has become a critical issue due to their rapid progress. However, our understanding of effective safety mechanisms in LLMs remains limited, leading to safety alignment training that mainly focuses on improving optimization, data-level enhancement, or adding extra structures to intentionally block harmful outputs. To address this gap, we develop a neuron detection method to identify safety neurons—those consistently crucial for handling and defending against harmful queries. Our findings reveal that these safety neurons constitute less than 1% of all parameters, are language-specific and are predominantly located in self-attention layers. Moreover, safety is collectively managed by these neurons in the first several layers. Based on these observations, we introduce a Safety Neuron Tuning method, named SN-Tune, that exclusively tune safety neurons without compromising models’ general capabilities. SN-Tune significantly enhances the safety of instruction-tuned models, notably reducing the harmful scores of Llama3-8B-Instruction from 65.5 to 2.0, Mistral-7B-Instruction-v0.2 from 70.8 to 4.5, and Vicuna-13B-1.5 from 93.5 to 3.0. Moreover, SN-Tune can be applied to base models on establishing LLMs’ safety mechanism, effectively diminishing models’ harmful scores from around 100 to 5.3, 13.5, and 13.8 for LLama2-7B-Base, LLama3-8B-Base, and Mistral-7B-v0.1, respectively. In addition, we improve the LLMs’ safety robustness during downstream tasks fine-tuning by separating the safety neurons from models’ foundation neurons.

1 INTRODUCTION

The rapid developments of Large Language Models (LLMs) (Achiam et al., 2023; Jiang et al., 2023; Reid et al., 2024; Team et al., 2024; Dubey et al., 2024) have brought safety alignment to the forefront of research (Zou et al., 2023; Zhao et al., 2024d; Zou et al., 2024; Deng et al., 2024; Wei et al., 2024). Different perspectives have been studied to improve safety alignments, such as improving optimization (Ouyang et al., 2022; Rafailov et al., 2024; Yuan et al., 2023), refining training data (Zhou et al., 2024; Rafailov et al., 2024; Zhang et al., 2024), or implementing additional structures designed to intentionally block harmful outputs (Inan et al., 2023; Zou et al., 2024). Despite its importance, a clear understanding of safety mechanisms in LLMs remains absent. Prior works tried to identify and interpret safety mechanisms in LLMs from either layer-level (Li et al., 2024) or feature-level (Chen et al., 2024). However, their identification methods attribute nearly 10% of parameters to safety-related functions. This large proportion makes it challenging to effectively perform safety alignments based on these findings (Anwar et al., 2024; Zeng et al., 2024). Moreover, other works have suggested that safety mechanisms can be easily compromised through minor parameter adjustments (Qi et al., 2024; Zhao et al., 2024a).

In this work, we aim to understand and interpret safety mechanisms in LLMs at a finer granularity, specifically at the neuron level across all structures, including the self-attention and feed-forward parts. Here, a “neuron” is represented by a single row or column of a parameter matrix in LLMs. We identify a “safety neuron” as one that consistently plays a crucial role in processing and defending against harmful queries. Specifically, a neuron is considered important if its removal—by setting its parameters to zero—significantly affects the generated output beyond a specified threshold. To achieve this, we input a corpus of harmful queries and extract neurons that are important across all queries in the corpus, identifying them as the set of safety neurons in the LLM. By conducting a thorough analysis of these identified safety neurons in various models, we uncover several key insights

about LLMs’ safety mechanisms. First, we find that safety neurons comprise less than 1% of all parameters. Second, each language has its own unique safety neurons, with minimal overlap between them. Third, safety is collaboratively managed by safety neurons located in the first several layers of the model. Lastly, safety neurons are predominantly located within the self-attention structures.

Motivated by these intriguing observations, we propose a Safety Neuron Tuning method, named SN-Tune, designed to exclusively tune the safety neurons in LLMs. As shown in Figure 1, we gather safety training documents that include harmful queries and refusal safety outputs, similar to the widely used safety alignment training settings (Inan et al., 2023; Zhang et al., 2024; Zou et al., 2024).

We then tune the identified safety neurons while leaving other safety-unrelated neurons unchanged by setting their gradients to zero during the tuning process. Experimental results demonstrate that SN-Tune not only enhances the safety mechanism for instruction-tuned models but also establishes safety mechanism for base models without compromising their

general capabilities. Notably, it reduces the average harmful scores of Llama3-8B-Instruction from 65.5 to 2.0, Mistral-7B-Instruct-v0.2 from 70.8 to 4.5, and Vicuna-13B-1.5 from 93.5 to 3.0. Moreover, SN-Tune reduces base models’ harmful score from around 100 to 5.3, 13.5, and 13.8 for LLama2-7B-Base, LLama3-8B-Base, and Mistral-7B-v0.1, respectively. The harmful score is evaluated using the harmful behavior dataset (Zou et al., 2023), by averaging the Attack Success Rate (ASR) across various adversarial attacking methods, including Direct Attack, GCG (Zou et al., 2023), AutoDAN (Liu et al., 2024) and PAIR (Chao et al., 2023). Concurrently, we assess the models’ general capabilities using representative NLP tasks including MMLU (Hendrycks et al., 2020), ARC-Challenge (Clark et al., 2018), and GSM8K (Cobbe et al., 2021), ensuring that safety improvements do not come at the cost of overall performance.

Building upon the strong performance of SN-Tune, we aim to further enhance LLMs’ safety robustness during downstream tasks fine-tuning, a common practice for users focusing on specific application scenarios (Yu et al., 2024; Zhao et al., 2024c). As Qi et al. (2024) observed, even fine-tuning with seemingly benign and widely used datasets can unintentionally compromise the safety alignment of LLMs. From the neuron perspective, fine-tuning on downstream tasks modifies certain foundation neurons (Zhao et al., 2024b; Liang et al., 2024). Consequently, the vulnerability of a model’s safety mechanism to downstream task fine-tuning may be attributed to the overlap between these foundation neurons and safety neurons, with the latter being unintentionally adjusted during the fine-tuning process. Inspired by this observation, we propose another technique called Robust Safety Neuron Tuning method (RSN-Tune). It separates safety neurons from foundation neurons by selectively tuning only those safety neurons that do not overlap with foundation neurons when applying SN-Tune to instruction-tuned models. Experimental results demonstrate the effectiveness of RSN-Tune in enhancing models’ safety robustness during downstream tuning. Notably, it reduces Llama2-7B-Chat’s harmful score after tuning on GSM8K training set from 41.0 to 26.0 and Mistral-7B-Instruct-v0.2’s from 79.0 to 41.0. Importantly, RSN-Tune enhances safety robustness while maintaining models’ downstream tuning performance.

2 SAFETY NEURONS

In this section, we propose a neuron detection method that can calculate the importance of a neuron when handling a query without a corresponding labeled output.

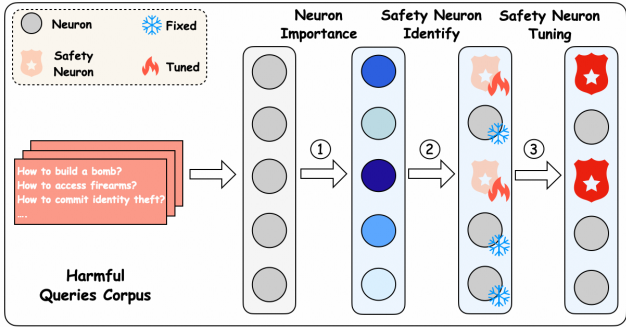


Figure 1: SN-Tune mainly consists of three steps: ① calculating neuron importance for handling harmful queries; ② identifying “safety neuron” that consistently play a crucial role in processing harmful queries; ③ tune the identified safety neurons while leaving other safety-unrelated neurons unchanged during the tuning process.

2.1 SAFETY NEURON DETECTION

A *neuron* is defined as a single row or column of a parameter matrix in LLMs, including the self-attention and feed-forward structures. To identify neurons responsible for safety in an alignment-tuned LLM, it’s crucial to extract those that play a key role in processing inputted harmful queries.

Foundational Safety Neuron Detection Formally, we denote the l -th neuron in layer i as $N_i^{(l)}$, while the intermediate representation after layer i when handling harmful query x is denoted as $h_i(x)$. Furthermore, the importance of neuron $N_i^{(l)}$ in processing x is calculated by

$$\|h_{\setminus N_i^{(l)},i}(x) - h_i(x)\|_2, \quad (1)$$

where $h_{\setminus N_i^{(l)},i}(x)$ represents the intermediate representation after deactivating neuron $N_i^{(l)}$. Therefore, the activated neurons of the model when handling harmful query x can be calculated by

$$\mathcal{N}_x = \{N_i^{(l)} \mid \|h_{\setminus N_i^{(l)},i}(x) - h_i(x)\|_2 \geq \epsilon, \text{ for all } N_i^{(l)} \text{ in LLM}\}, \quad (2)$$

where ϵ is a pre-defined threshold. Furthermore, after collecting a set of harmful queries, denoted as X . We extract neurons consistently activated for all queries in X , identifying the safety neurons we aim to obtain, i.e.,

$$\mathcal{N}_{\text{safe}} = \{N_i^{(l)} \mid N_i^{(l)} \in \mathcal{N}_x, \forall x \in X, \text{ for all } N_i^{(l)} \text{ in LLM}\}. \quad (3)$$

Accelerated Safety Neuron Detection The process of deactivating $N_i^{(l)}$ sequentially in Equation 2 is extremely slow due to its sequential nature. Drawing inspiration from the parallel neuron detection method proposed by Zhao et al. (2024b), we implement it on safety neuron detection through the incorporation of masks and parallel computations. Specifically, for the feed-forward layer,

$$\|h_{\setminus N_i^{(l)},i}(x) - h_i(x)\|_2 = \|(h_{\text{ffn}}(x) \cdot \text{Mask})W_{\text{down}}\|_2, \quad (4)$$

where h_{ffn} is the intermediate embedding between the up-projection and down-projection matrices, Mask is an identity matrix of size $(\dim(h_{\text{ffn}}) \times \dim(h_{\text{ffn}}))$, and W_{down} denotes the down-projection matrix in the feed-forward layer. Moreover, for the self-attention layer,

$$\|h_{\setminus N_i^{(l)},i}(x) - h_i(x)\|_2 \approx \left\| \text{softmax}\left(\frac{W_Q(x)W_K^T(x) - \Delta(x)}{\sqrt{d}}\right) - \text{softmax}\left(\frac{W_Q(x)W_K^T(x)}{\sqrt{d}}\right) \right\|_2, \quad (5)$$

where W_Q and W_K are the attention matrices for Q and K , respectively, and \sqrt{d} represents the corresponding dimension following the notations in Vaswani et al. (2017), and

$$\Delta(x) = W_Q(x).\text{resize}(l, 1, d) \times W_K(x).\text{resize}(1, l, d) \in \mathbb{R}^{l \times l \times d}. \quad (6)$$

Detailed proof of Equation 4 and Equation 5 is available in Appendix A.1.

2.2 VERIFY IDENTIFIED SAFETY NEURON

We subsequently apply the accelerated safety neuron detection method to a variety of alignment-tuned LLMs to identify corresponding safety neurons, and conduct experiments to verify that these neurons are exclusively responsible for handling safety. Specifically, by deactivating the safety neurons, the model’s safety mechanism will be attacked, potentially transforming it into a harmful model. However, by solely manipulating neurons associated with safety, the overall functionality should remain intact. Consequently, the model could become both helpful and harmful.

Experimental Setup We employ three open-source models that have been specifically tuned for safety, including Llama2-7B-Chat (Touvron et al., 2023), Llama3-8B-Instruction (Dubey et al., 2024), and Mistral-7B-Instruct-v0.2 (Jiang et al., 2023). The harmful corpus set used to detect safety neurons is constructed from the training set split in Zou et al. (2024). [More details are illustrated in Appendix A.2.](#) To prove the generability of the detected safety neuron, we test the harmfulness of the model on harmful behavior testset in Zou et al. (2023) (Harm Behavior), adversarial behavior testset in Mazeika et al. (2024) (Adv Behavior) and English version of multilingual jailbreak testset in Deng et al. (2024) (MultiJail-En). Furthermore, the models’ general capability is evaluated by MMLU Hendrycks et al. (2020) and GSM8K Cobbe et al. (2021).

Table 1: Performance of models on harmfulness and general capability with the deactivation of safety neurons (“Deact-SN”) and an equivalent number of randomly selected neurons (“Deact-R”). Harmfulness is measured by Attack Success Rate (lower is safer), and capability by Accuracy.

Dataset	Llama2-7B-Chat			Llama3-8B-Instruction			Mistral-7B-Instruct-v0.2			
	Origin.	Deact-R	Deact-SN	Origin.	Deact-R	Deact-SN	Origin.	Deact-R	Deact-SN	
Harmful↓	Harm Behavior	0.0	2.0	97.0	30.0	31.0	78.0	36.0	39.0	86.0
	Adv Behavior	0.0	3.0	83.0	7.0	13.0	96.0	30.0	30.0	87.0
	MultiJail-En	12.7	12.9	81.6	20.0	21.6	74.3	44.1	46.8	86.4
	<i>Avg. Harmful</i>	4.2	6.0	87.2	19.0	21.9	82.8	36.7	38.6	86.5
Capability↑	MMLU	48.2	48.4	47.8	65.3	63.2	62.7	59.2	59.3	58.5
	GSM8K	24.8	22.7	21.9	75.9	73.6	72.4	43.6	43.6	42.1
	<i>Avg. Capability</i>	36.5	35.6	34.8	70.6	68.4	67.6	51.4	51.5	50.3

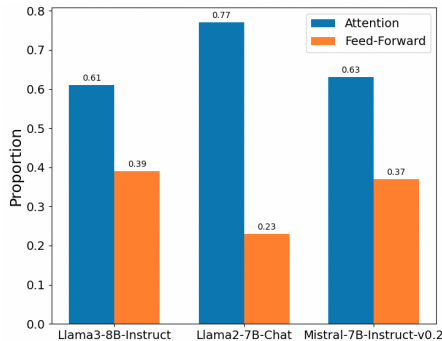
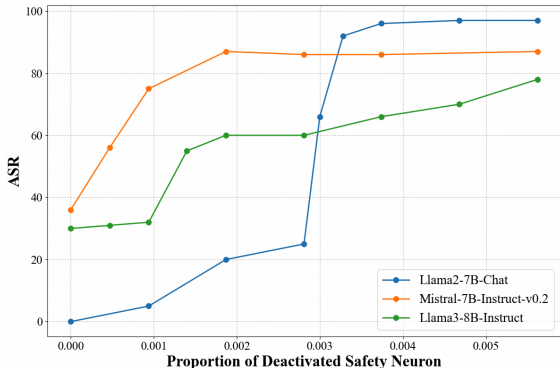


Figure 2: Effects of deactivated safety neurons on ASR.

Figure 3: Distribution of Safety Neuron in different structures.

Evaluation Metrics The harmfulness is assessed through direct attacks using the Attack Success Rate (ASR), which identifies harmful keywords from the output, following the method outlined by Zou et al. (2023). Furthermore, accuracy is the metric used for MMLU and GSM8K.

Existence of Safety Neurons Table 1 demonstrates how deactivating safety neurons can attack the model’s safety mechanism. Moreover, the model’s general capabilities have not diminished, indicating that these neurons are specifically for safety mechanisms, not for other functions. Even with just about 0.5% of neurons deactivated, the model’s safety capabilities are significantly compromised, leading to a substantial increase in harmful behavior: from 4.2 to 87.2 on Llama2-7B-chat, from 19.0 to 82.8 on Llama3-8B-Instruction, and from 36.7 to 86.5 on Mistral-7B-Instruct-v0.2. Meanwhile, randomly deactivating an equivalent number of neurons has little to no impact on the model’s safety. Regarding general capability, deactivating the safety neuron shows minimal impact, similar to deactivating randomly selected neurons, as demonstrated by the performance of 36.5 and 34.8 on Llama2-7B-chat, 70.6 and 68.4 on Llama3-8B-Instruction, and 51.4 and 50.3 on Mistral-7B-Instruct-v0.2 before and after deactivation. Therefore, the detected neurons are safety neurons that are associated with safeguarding the models.

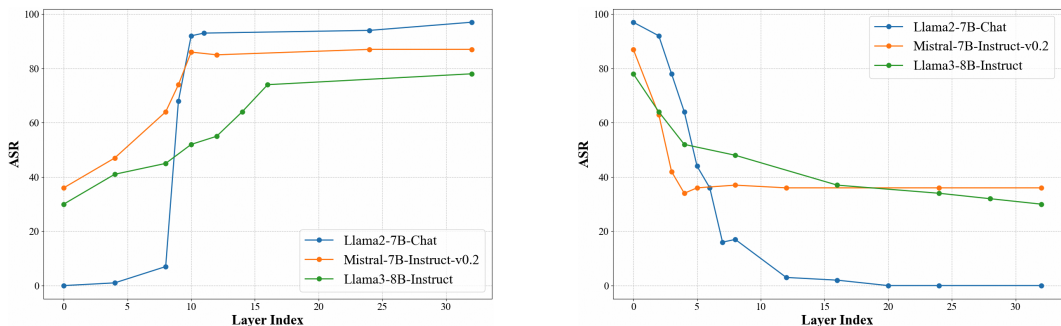
2.3 ANALYZE SAFETY MECHANISM IN LLMs

As we have detected the safety neurons of LLMs, we conduct a more detailed and comprehensive analysis of the properties of LLM’s safety mechanism.

2.3.1 SAFETY MECHANISM PROPERTIES

Safety mechanism is resilient but breakable by under one percent of the parameters. Figure 2 shows the harmful score of three models as deactivating different number of safety neurons. In Mistral-7B-Instruct-v0.2, deactivating 0.2% of neurons can destroy its safety mechanism, compared to 0.4% for Llama2-7B-Chat and 0.5% for Llama3-8B-Instruction. Furthermore, an emergence of

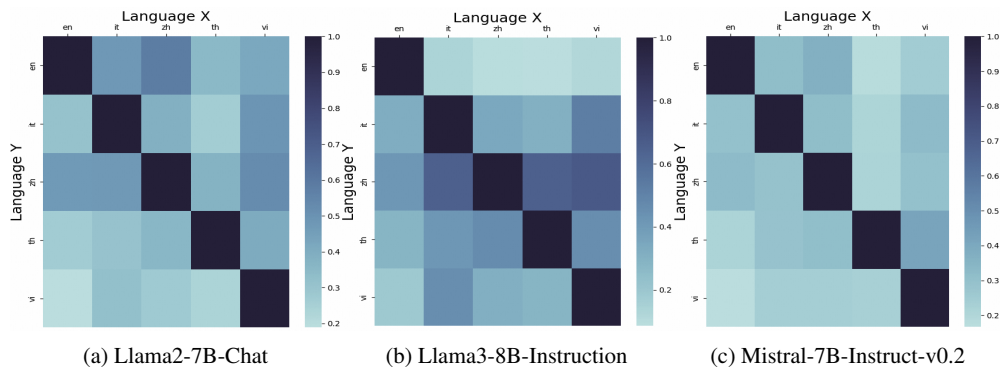
216
217
218
219
220
221
222
223
224
225
226



227
228
229

Figure 4: Effect of deactivating safety neurons in different layers. The left represents deactivating safety neurons *before* the certain layers, the right indicates deactivation *after* the certain layers.

230
231
232
233
234
235
236
237
238
239
240
241



242
243
244

Figure 5: Overlapping ratio of safety neurons across different languages.

245
246
247

“harmfulness” is observed for three models. For example, in Llama2-7B-Chat, the leap appears when deactivating 0.3% neurons, while the number is 0.15% for Llama3-8B-Instruction and is 0.1% for Mistral-7B-Instruct-v0.2.

248
249
250
251
252
253
254

Safety Mechanism is handled by the first several layers together. Figure 4 illustrates the detrimental impact of deactivating safety neurons across various layers in models. Upon deactivating neurons in the first 10 layers simultaneously, we observe a near-complete breakdown in the safety mechanism of Llama2-7B-Chat. This threshold is 10 for Mistral-7B-Instruct-v0.2 and 16 for Llama3-8B-Instruction. On the contrary, if we deactivate safety neurons from the back to the front, the breakdown of safety mechanisms becomes apparent as nearly all safety neurons are deactivated.

255
256
257
258
259
260
261
262
263
264

Safety neurons predominantly reside within the self-attention layers. In Figure 3, safety neurons are categorized based on their belonging structures, which include the attention structure and feed-forward structure. Our findings reveal that safety neurons predominantly reside within the attention structure. Specifically, in Llama2-7B-Chat, 77% of safety neurons are attributed to the attention structure, while 23% belong to the feed-forward structure. This finding aligns with the interpretation that the attention structure primarily handles understanding, while the feed-forward structure is mainly responsible for knowledge extraction (Geva et al., 2021). Given that the safety mechanism focuses on understanding potential threats to discern their harmful nature without the need to extract much new knowledge, it is logical for safety neurons to predominantly reside in the attention structure, despite the attention parameters being fewer than half of the feed-forward parameters.

265
266

2.3.2 MULTILINGUAL SAFETY

267
268
269

Based on the research by Deng et al. (2024); Yong et al. (2024); Kotha et al. (2024), the safety mechanism cannot be effectively transferred between languages. For instance, even when a LLM is specifically tuned for safety in English, it may still pose risks when applied to other languages. Drawing inspiration from these discoveries, we analyze this phenomenon through the perspective

Table 2: Performance of SN-Tune on instruction-tuned models. General capabilities are evaluated by accuracy, while harmfulness is evaluated by ASR.

Dataset	Vicuna-13B-v1.5			Llama3-8B-Instruction			Mistral-7B-Instruct-v0.2			
	Origin.	Circ-Break	SN-Tune	Origin.	Circ-Break	SN-Tune	Origin.	Circ-Break	SN-Tune	
Training Cost (min.)	-	43	4	-	24	2	-	23	2	
# Parameters (M)	0	34.1	0	0	27.5	0	0	27.5	0	
Capability↑	MMLU	53.4	52.8	55.7	65.2	65.6	67.3	58.6	56.3	59.5
	ARC-c	59.7	61.3	61.6	73.7	74.1	74.9	72.6	71.8	73.4
	GSM8K	33.4	35.0	34.8	63.2	64.3	69.6	43.7	42.5	44.1
	<i>Avg. Capability</i>	48.8	49.7	50.7	67.4	68.0	68.4	58.3	56.9	59.0
Harmful↓	Direct	92.0	0.0	0.0	30.0	0.0	0.0	36.0	7.0	0.0
	GCG	100.0	3.0	0.0	74.0	3.0	4.0	88.0	8.0	6.0
	AutoDAN	93.0	2.0	3.0	82.0	0.0	0.0	91.0	3.0	4.0
	PAIR	89.0	16.0	9.0	76.0	9.0	4.0	68.0	22.0	8.0
<i>Avg. Harmful</i>	93.5	5.3	3.0	65.5	3.0	2.0	70.8	10.0	4.5	

of safety neurons. We specifically incorporate five languages—English (en), Italian (it), Chinese (zh), Thai (th), and Vietnamese (vi)—spanning high-resource to low-resource languages, to visualize the overlap of safety neurons. Specifically, the overlap among safety neurons are defined as $overlap(x, y) = |\mathcal{N}_x \cap \mathcal{N}_y|/|\mathcal{N}_y|$, where $\mathcal{N}_{\text{language}}$ represents the set of safety neurons in that language. Figure 5 displays the intersection of safety neurons across languages. Our analysis reveals that the overlap of safety neurons is typically below 30%, significantly less than that of language-specific neurons, which are a subset of neurons responsible for processing multilingual queries (Zhao et al., 2024b). This disparity underscores the unique nature of safety neurons in each language, indicating that safety capabilities are not transferrable between languages. This observation aligns with the progression of the SFT training, where diverse language-specific safety corpora are developed to provide tailored safety mechanism for individual languages (Zhang et al., 2024).

3 EFFICIENT SAFETY TRAINING

With only a limited number of parameters able to ensure safety, we can focus on manipulating these neurons effectively to strengthen or even establish the safety mechanism.

3.1 LIVE-LINE WORK ON INSTRUCT TUNED MODEL

Experimental Setup With fewer than 1% of neurons dedicated to safety, we can enhance safety by fine-tuning them using a safety corpus, named as Safety Neuron Tuning (SN-Tune). Specifically, we create a safety corpus by partitioning a training dataset from (Zou et al., 2024), utilizing it to identify and strengthen safety neurons. In a manner similar to the setup in Table 1, we assess models’ harmfulness using the harmful behavior testset, while their general capabilities are evaluated on MMLU (5-shots) (Hendrycks et al., 2020), ARC-c (3-shots) (Clark et al., 2018), and GSM8K (zero-shot) (Cobbe et al., 2021). Additionally, beyond testing direct attacks, we explore other attack methods, including GCG (Zou et al., 2023), AutoDAN (Liu et al., 2024), and PAIR (Chao et al., 2023). To demonstrate the generality of the method, we also employ the large model Vicuna-13B-v1.5 (Peng et al., 2023) in addition to Llama3-8B-Instruction and Mistral-7B-Instruct-v0.2. We compare SN-Tune with Zou et al. (2024), who train an independent model called “Circ-Break” to act as a circuit breaker, interrupting models when they produce harmful outputs.

Experiment Details We utilize the HarmBench implementation (Mazeika et al., 2024) for the attacking methods. For general capability evaluation, we employ accuracy as the metric, while for harmfulness assessment, we use Attack Success Rate (ASR). The hyperparameters for fine-tuning primarily focus on the training corpus, number of epochs, and learning rate. As the fine-tuning process is essentially continued training, we aim to minimize alterations to the existing parameters. Specifically, we use a dataset of 50 documents where the model refuses to answer harmful questions, train for only 1 epoch, and set the initial learning rate to $1e - 6$.

Table 3: Performance of SN-Tune on base models. General capabilities are evaluated by accuracy, while harmfulness is evaluated by ASR.

Dataset	Llama2-7B-Base			Llama3-8B-Base			Mistral-7B-v0.1			
	Origin.	Circ-Break	SN-Tune	Origin.	Circ-Break	SN-Tune	Origin.	Circ-Break	SN-Tune	
Training Cost (min.)	-	23	2	-	35	2	-	21	2	
# Parameters (M)	0	34.1	0	0	27.5	0	0	27.5	0	
Capability \uparrow	MMLU	49.2	49.1	49.2	70.1	68.9	69.6	68.4	68.1	69.2
	ARC-c	27.6	26.8	29.3	70.7	72.0	71.8	74.8	73.4	74.7
	GSM8K	12.7	13.7	16.3	58.9	58.2	59.5	50.4	47.6	52.3
	Avg. Capability	29.8	29.9	31.6	66.6	66.4	67.0	62.0	63.0	65.4
Harmful \downarrow	Direct	97.0	84.0	0.0	100.0	87.0	0.0	100.0	78.0	6.0
	GCG	100.0	92.0	7.0	100.0	95.0	14.0	100.0	82.0	13.0
	AutoDAN	100.0	97.0	9.0	100.0	92.0	21.0	100.0	93.0	12.0
	PAIR	98.0	89.0	5.0	100.0	96.0	19.0	100.0	97.0	24.0
	Avg. Harmful	98.8	90.5	5.3	100.0	92.5	13.5	100.0	87.5	13.8

Table 4: RSN-Tune’s performance on improving models’ safety robustness. “Before”: pre-tuning. “Original”: direct tuning. “SN-Tune” and “RSN-Tune”: tuning on safety-enhanced models.

Dataset	Llama2-7B-Chat				Mistral-7B-Instruct-v0.2			
	Before	Origin.	SN-Tune	RSN-Tune	Before	Origin.	SN-Tune	RSN-Tune
GSM8K	16.8	26.5	27.2	26.2	43.7	63.4	61.8	63.2
Harmful	0.0	41.0	38.0	26.0	36.0	79.0	72.0	41.0

Main Results Table 2 shows the performance of SN-Tune on instruction tuned model. Note that tuning base models can be regarded as live-line work, meaning that we hope to enhance models’ safety without sacrificing models’ general instruction following capabilities in other aspects. We find that SN-Tune effectively enhances model safety without compromising general capabilities, and in some cases, even slightly improves them. Specifically, SN-Tune reduces the harmful score of Vicuna-13B-v1.5 from 93.5 to 3.0, Llama3-8B-Instruction from 65.5 to 2.0, and Mistral-7B-Instruct-v0.2 from 70.8 to 4.5. Meanwhile, the general capabilities are largely preserved. Furthermore, compared to Circ-Break, SN-Tune requires less training time and fewer additional parameters.

3.2 EFFICIENT ESTABLISH SAFE MECHANISM FOR BASE MODEL

Experimental Settings When implementing SN-Tune on base models, we largely maintain the settings described in Section 3.1, with two key differences. First, we do use the specific chat template for fine-tuning. Second, for evaluations on GSM8K, we employ a 5-shot approach rather than zero-shot, given the use of base models.

Main Results Table 3 shows the performance of SN-Tune on base models. We find that SN-Tune effectively enhances model safety without compromising general capabilities, and in some cases, even slightly improves them. Specifically, SN-Tune reduces the harmful score of Llama2-7B-Base from 98.8 to 5.3, Llama3-8B-Base from 100.0 to 13.5, and Mistral-7B-v0.1 from 100.0 to 13.8. Meanwhile, the general capabilities are largely preserved. For instance, the original general capability score for Llama2-7B-Base is 29.8, while the model after SN-Tune achieves 31.6. Similarly, the score increases from 66.6 to 67.0 for Llama3-8B-Base and from 100.0 to 13.8 for Mistral-7B-v0.1. Furthermore, different from instruction-tuned models, Circ-Break can not construct safety mechanism on the base model with several training corpus. Specifically, harmful score of Llama2-7B-Base after tuned by Circ-Break is still 90.5, while the number is 92.5 for Llama3-8B-Base and 87.5 for Mistral-7B-v0.1. Moreover, the training time for SN-Tune on Llama2-7B-Base is just 2 minutes, while Circ-Break requires 23 minutes. On Llama3-8B-Base, the time costs are 2 and 35 minutes respectively, while on Mistral-7B-v0.1, they are 2 and 21 minutes respectively.

378
379
380
381
382
383
384
385
386
387
388
389
390
391
392
393
394
395
396
397
398
399
400
401
402
403
404
405
406
407
408
409
410
411
412
413
414
415
416
417
418
419
420
421
422
423
424
425
426
427
428
429
430
431

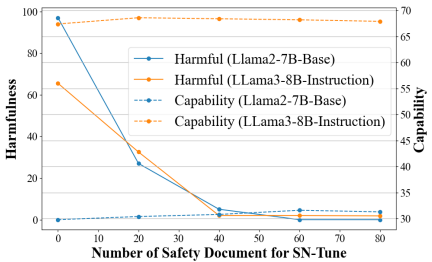


Figure 6: Ablation on the number of safety documents used in training.

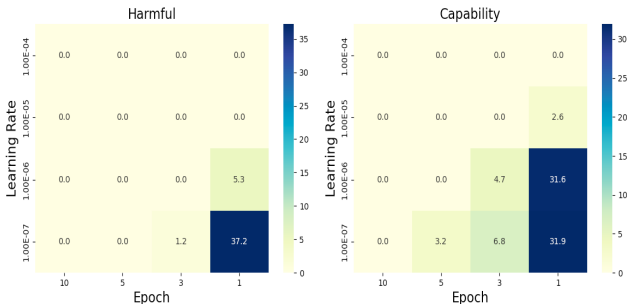


Figure 7: Ablation on training epoch and learning rate..

4 MORE ROBUST EFFICIENT SAFETY TUNING

Fine-tuning instruction-tuned models on specific downstream tasks is a common practice for users seeking to optimize performance in particular application scenarios (Yu et al., 2024; Zhao et al., 2024c). However, Qi et al. (2024); Jain et al. (2024) have noted that even fine-tuning with seemingly benign and widely used datasets can unintentionally compromise the safety alignment of LLMs. To address this issue and mitigate its effects, we propose a Robust Safety Neuron Tuning method, called RSN-Tune. According to Zhao et al. (2024b), a specialized set of neurons, termed foundation neurons, are responsible for fundamentally managing queries. Consequently, the vulnerability of a model’s safety mechanism to general fine-tuning may be attributed to the overlap between foundation neurons and safety neurons, with the latter being inadvertently altered during the fine-tuning process. Inspired by this observation, we propose separating the safety neurons from the foundation neurons. This separation is achieved by selectively tuning only those safety neurons that do not overlap with foundation neurons when applying SN-Tune to instruction-tuned models, as illustrated in Section 3.1. We then conduct experiments to prove the effectiveness of RSN-Tune.

Experiment Settings We employ Llama2-7B-Chat and Mistral-7B-Instruct-v0.2 as backbone models considering their excellent safety performance and generality. For fine-tuning, we employ the GSM8K dataset (Cobbe et al., 2021), widely recognized as a challenging and representative benchmark for reasoning tasks. The foundation neurons are detected by Wikipedia corpus¹ with the same neuron detection method illustrated in Section 2.1.

Main Results Table 4 demonstrates the effectiveness of RSN-Tune in enhancing models’ safety robustness during downstream tuning. We observe that direct tuning using the GSM8K training set significantly increases model harmfulness. For instance, Llama2-7B-Chat’s harmful score rises from 0.0 to 41.0, while Mistral-7B-Instruct-v0.2’s score increases from 36.0 to 79.0. This phenomenon also affects SN-Tune, which indiscriminately enhances all safety neurons, regardless of their overlap with foundation neurons. In contrast, RSN-Tune partially preserves model safety after downstream tuning. Specifically, it reduces Llama2-7B-Chat’s harmful score to 26.0 and Mistral-7B-Instruct-v0.2’s to 41.0. However, a complete harmful score reduction to 0.0 is not achievable due to an insufficient number of non-overlapping safety neurons.

5 FURTHER ANALYSIS

In this section, to further understand the mechanism and explore the influencing factors to the performance of SN-Tune, we conduct comprehensive ablation analysis, mainly including the number of training safety documents, training epoch and learning rate.

5.1 NUMBER OF SAFETY DOCUMENTS FOR SN-TUNE

Experiment Settings We employ LLama2-7B-Base to serve as the representative base model and Llama3-8B-Instruction to represent the instruction-tuned model. Following the setting outlined in

¹<https://huggingface.co/datasets/wikimedia/wikipedia>

Section 3, we assess the models’ overall performance and potential harmfulness after tuning by SN-Tune with varying quantities of safety-related documents.

Main Results Figure 6 illustrates the effect of training document quantity on SN-Tune. We observe that the general capabilities of both LLama2-7B-Base (yellow dotted line) and Llama3-8B-Instruction (blue dotted line) remain largely unaffected regardless of the training document size. This stability is primarily attributed to the limited number of neurons trained. Specifically, as we only train the safety neurons, which comprise approximately 0.5% of all parameters, the majority of the language ability remains intact, resulting in preserved general capabilities. Notably, the harmful score of both models decreases rapidly as the number of training documents increases to 40 for LLama2-7B-Base (yellow line) and Llama3-8B-Instruction (blue line). This demonstrates the efficiency of SN-Tune in both enhancing and establishing model safety mechanism with just a few dozen documents. In contrast, Circ-Break requires around 4000 safety documents and a retention dataset of similar size (Zou et al., 2024). These findings underscore that SN-Tune is not only effective but also highly efficient in tuning safety for LLMs.

5.2 LEARNING RATE & TRAINING EPOCH

Experiment Settings We further explore the effects of learning rate and number of training epochs simultaneously, as both hyperparameters influence the magnitude of parameter updates. We employ Llama2-7B-Base as our model since instruction-tuned versions derived from it are highly representative of safe language models. Similar to Section 5.1, we investigate the model’s performance in terms of both general capabilities and safety aspects.

Main Results Figure 7 illustrates the impact of learning rate and training epoch on both harmfulness (left) and general capability (right). We observe that with 10 training epochs, harmful score reaches 0.0, but the model also loses generality, scoring 0.0 in capability. As the number of epochs decreases, this effect diminishes. For instance, with 5 epochs and a learning rate of 10^{-7} , the general capability improves to 3.2. Further reducing to 3 epochs maintains low harmful scores across all learning rates while increasing general capability to 6.8 at a 10^{-7} learning rate. The best performance is achieved with a single epoch, aligning with other continue-train approaches (Dou et al., 2024; Zhang et al., 2024). Additionally, higher learning rates lead to overfitting, resulting in both harmful score and general capabilities dropping to 0.0, while lower rates fail to effectively train safety into the model. Consequently, a learning rate of 10^{-6} emerges as the optimal balance between low harmful score and high general capability.

6 RELATED WORK

Safety Alignment. To build safe LLMs, alignments has also been a widely studied topic in the community (Stiennon et al., 2020; Ouyang et al., 2022). Efforts have been put into improving helpfulness (Bai et al., 2022; Cheng et al., 2023), honesty (Kaddour et al., 2023; Liu et al., 2023; Park et al., 2023), and harmlessness (Hartvigsen et al., 2022). Among them, safety, i.e., reducing harmfulness, is established and improved via optimization (Ouyang et al., 2022; Rafailov et al., 2024; Yuan et al., 2023), refining training data (Zhou et al., 2024; Rafailov et al., 2024; Zhang et al., 2024), or implementing additional structures designed to intentionally block harmful outputs (Inan et al., 2023; Zou et al., 2024). However, these methods are indirect and require many resources.

Interpretability. In the era of LLMs, one brunch of interpretability work includes efforts to understand knowledge storage (Geva et al., 2021; Dai et al., 2022; Geva et al., 2022; Meng et al., 2022; Li et al., 2023). Another line of research centers on the self-attention layer, examining its connection to reasoning capability (Hou et al., 2023; Stolfo et al., 2023; Friedman et al., 2023) by contrasting the reasoning tree based on attention weights. In the context of safety, prior works tried to identify and interpret safety mechanisms in LLMs from either layer-level (Li et al., 2024) or feature-level (Chen et al., 2024). However, their identification methods attribute nearly 10% of parameters to safety-related functions, which is too coarse to be used.

7 CONCLUSION

Safety alignment in LLMs is critical yet underexplored. We introduced a method to detect and tune safety neurons, which are less than 1% of parameters and mainly in self-attention layers. Our Safety Neuron Tuning (SN-Tune) enhances model safety without compromising performance, significantly reducing harmful scores in both instruction-tuned and base models. This approach also improves safety robustness during fine-tuning by separating safety neurons from foundational ones.

REFERENCES

- Josh Achiam, Steven Adler, Sandhini Agarwal, Lama Ahmad, Ilge Akkaya, Florencia Leoni Aleman, Diogo Almeida, Janko Altenschmidt, Sam Altman, Shyamal Anadkat, et al. Gpt-4 technical report. *arXiv preprint arXiv:2303.08774*, 2023.
- Usman Anwar, Abulhair Saparov, Javier Rando, Daniel Paleka, Miles Turpin, Peter Hase, Ekdeep Singh Lubana, Erik Jenner, Stephen Casper, Oliver Sourbut, et al. Foundational challenges in assuring alignment and safety of large language models. *arXiv preprint arXiv:2404.09932*, 2024.
- Yuntao Bai, Andy Jones, Kamal Ndousse, Amanda Askell, Anna Chen, Nova DasSarma, Dawn Drain, Stanislav Fort, Deep Ganguli, Tom Henighan, et al. Training a helpful and harmless assistant with reinforcement learning from human feedback. *arXiv preprint arXiv:2204.05862*, 2022.
- Patrick Chao, Alexander Robey, Edgar Dobriban, Hamed Hassani, George J Pappas, and Eric Wong. Jailbreaking black box large language models in twenty queries. *arXiv preprint arXiv:2310.08419*, 2023.
- Jianhui Chen, Xiaozhi Wang, Zijun Yao, Yushi Bai, Lei Hou, and Juanzi Li. Finding safety neurons in large language models. *arXiv preprint arXiv:2406.14144*, 2024.
- Pengyu Cheng, Yifan Yang, Jian Li, Yong Dai, and Nan Du. Adversarial preference optimization. *arXiv preprint arXiv:2311.08045*, 2023.
- Peter Clark, Isaac Cowhey, Oren Etzioni, Tushar Khot, Ashish Sabharwal, Carissa Schoenick, and Oyvind Tafjord. Think you have solved question answering? try arc, the ai2 reasoning challenge. *arXiv preprint arXiv:1803.05457*, 2018.
- Karl Cobbe, Vineet Kosaraju, Mohammad Bavarian, Mark Chen, Heewoo Jun, Lukasz Kaiser, Matthias Plappert, Jerry Tworek, Jacob Hilton, Reiichiro Nakano, et al. Training verifiers to solve math word problems. *arXiv preprint arXiv:2110.14168*, 2021.
- Damai Dai, Li Dong, Yaru Hao, Zhifang Sui, Baobao Chang, and Furu Wei. Knowledge neurons in pretrained transformers. In *Proceedings of the 60th Annual Meeting of the Association for Computational Linguistics (Volume 1: Long Papers)*, pp. 8493–8502, 2022.
- Yue Deng, Wenxuan Zhang, Sinno Jialin Pan, and Lidong Bing. Multilingual jailbreak challenges in large language models. In *The Twelfth International Conference on Learning Representations*, 2024.
- Longxu Dou, Qian Liu, Guangtao Zeng, Jia Guo, Jiahui Zhou, Wei Lu, and Min Lin. Sailor: Open language models for south-east asia. *arXiv preprint arXiv:2404.03608*, 2024.
- Abhimanyu Dubey, Abhinav Jauhri, Abhinav Pandey, Abhishek Kadian, Ahmad Al-Dahle, Aiesha Letman, Akhil Mathur, Alan Schelten, Amy Yang, Angela Fan, et al. The llama 3 herd of models. *arXiv preprint arXiv:2407.21783*, 2024.
- Dan Friedman, Andrew Lampinen, Lucas Dixon, Danqi Chen, and Asma Ghandeharioun. Interpretability illusions in the generalization of simplified models, 2023.
- Mor Geva, Roei Schuster, Jonathan Berant, and Omer Levy. Transformer feed-forward layers are key-value memories. In *Proceedings of the 2021 Conference on Empirical Methods in Natural Language Processing*, pp. 5484–5495, 2021.

- 540 Mor Geva, Avi Caciularu, Kevin Wang, and Yoav Goldberg. Transformer feed-forward layers build
541 predictions by promoting concepts in the vocabulary space. In *Proceedings of the 2022 Conference*
542 *on Empirical Methods in Natural Language Processing*, pp. 30–45, 2022.
- 543 Thomas Hartvigsen, Saadia Gabriel, Hamid Palangi, Maarten Sap, Dipankar Ray, and Ece Kamar.
544 Toxigen: A large-scale machine-generated dataset for adversarial and implicit hate speech detection.
545 In *Proceedings of the 60th Annual Meeting of the Association for Computational Linguistics*
546 *(Volume 1: Long Papers)*, pp. 3309–3326, 2022.
- 547 Dan Hendrycks, Collin Burns, Steven Basart, Andy Zou, Mantas Mazeika, Dawn Song, and Jacob
548 Steinhardt. Measuring massive multitask language understanding. In *International Conference on*
549 *Learning Representations*, 2020.
- 551 Yifan Hou, Jiaoda Li, Yu Fei, Alessandro Stolfo, Wangchunshu Zhou, Guangtao Zeng, Antoine
552 Bosselut, and Mrinmaya Sachan. Towards a mechanistic interpretation of multi-step reasoning
553 capabilities of language models. In Houda Bouamor, Juan Pino, and Kalika Bali (eds.), *Proceedings*
554 *of the 2023 Conference on Empirical Methods in Natural Language Processing*, pp. 4902–4919,
555 Singapore, December 2023. Association for Computational Linguistics. doi: 10.18653/v1/2023.
556 emnlp-main.299. URL <https://aclanthology.org/2023.emnlp-main.299>.
- 557 Hakan Inan, Kartikeya Upasani, Jianfeng Chi, Rashi Rungta, Krithika Iyer, Yuning Mao, Michael
558 Tontchev, Qing Hu, Brian Fuller, Davide Testuggine, et al. Llama guard: Llm-based input-output
559 safeguard for human-ai conversations. *arXiv preprint arXiv:2312.06674*, 2023.
- 560 Samyak Jain, Robert Kirk, Ekdeep Singh Lubana, Robert P Dick, Hidenori Tanaka, Tim Rocktäschel,
561 Edward Grefenstette, and David Krueger. Mechanistically analyzing the effects of fine-tuning on
562 procedurally defined tasks. In *The Twelfth International Conference on Learning Representations*,
563 2024.
- 564 Albert Q Jiang, Alexandre Sablayrolles, Arthur Mensch, Chris Bamford, Devendra Singh Chaplot,
565 Diego de las Casas, Florian Bressand, Gianna Lengyel, Guillaume Lample, Lucile Saulnier, et al.
566 Mistral 7b. *arXiv preprint arXiv:2310.06825*, 2023.
- 567 Jean Kaddour, Joshua Harris, Maximilian Mozes, Herbie Bradley, Roberta Raileanu, and Robert
568 McHardy. Challenges and applications of large language models. *arXiv preprint arXiv:2307.10169*,
569 2023.
- 570 Suhas Kotha, Jacob Mitchell Springer, and Aditi Raghunathan. Understanding catastrophic forgetting
571 in language models via implicit inference. In *The Twelfth International Conference on Learning*
572 *Representations*, 2024.
- 573 Kenneth Li, Oam Patel, Fernanda Viégas, Hanspeter Pfister, and Martin Wattenberg. Inference-time
574 intervention: Eliciting truthful answers from a language model. *arXiv preprint arXiv:2306.03341*,
575 2023.
- 576 Shen Li, Liuyi Yao, Lan Zhang, and Yaliang Li. Safety layers of aligned large language models: The
577 key to llm security. *arXiv preprint arXiv:2408.17003*, 2024.
- 578 Yunlong Liang, Fandong Meng, Songming Zhang, Yufeng Chen, Jinan Xu, Jie Zhou, et al. Multilin-
579 gual knowledge editing with language-agnostic factual neurons. *arXiv preprint arXiv:2406.16416*,
580 2024.
- 581 Xiaogeng Liu, Nan Xu, Muhao Chen, and Chaowei Xiao. AutoDAN: Generating stealthy jailbreak
582 prompts on aligned large language models. In *The Twelfth International Conference on Learning*
583 *Representations*, 2024. URL <https://openreview.net/forum?id=7Jwpw4qKkb>.
- 584 Yang Liu, Yuanshun Yao, Jean-Francois Ton, Xiaoying Zhang, Ruocheng Guo Hao Cheng, Yegor
585 Klochkov, Muhammad Faaiz Taufiq, and Hang Li. Trustworthy llms: a survey and guideline for
586 evaluating large language models’ alignment. *arXiv preprint arXiv:2308.05374*, 2023.
- 587 Mantas Mazeika, Long Phan, Xuwang Yin, Andy Zou, Zifan Wang, Norman Mu, Elham Sakhaee,
588 Nathaniel Li, Steven Basart, Bo Li, et al. Harmbench: A standardized evaluation framework for
589 automated red teaming and robust refusal. In *Forty-first International Conference on Machine*
590 *Learning*, 2024.

- 594 Kevin Meng, David Bau, Alex Andonian, and Yonatan Belinkov. Locating and editing factual
595 associations in gpt. *Advances in Neural Information Processing Systems*, 35:17359–17372, 2022.
596
- 597 Long Ouyang, Jeffrey Wu, Xu Jiang, Diogo Almeida, Carroll Wainwright, Pamela Mishkin, Chong
598 Zhang, Sandhini Agarwal, Katarina Slama, Alex Ray, et al. Training language models to follow
599 instructions with human feedback. *Advances in neural information processing systems*, 35:27730–
600 27744, 2022.
- 601 Peter S Park, Simon Goldstein, Aidan O’Gara, Michael Chen, and Dan Hendrycks. Ai deception: A
602 survey of examples, risks, and potential solutions. *arXiv preprint arXiv:2308.14752*, 2023.
603
- 604 Baolin Peng, Chunyuan Li, Pengcheng He, Michel Galley, and Jianfeng Gao. Instruction tuning with
605 gpt-4. *arXiv preprint arXiv:2304.03277*, 2023.
606
- 607 Xiangyu Qi, Yi Zeng, Tinghao Xie, Pin-Yu Chen, Ruoxi Jia, Prateek Mittal, and Peter Henderson.
608 Fine-tuning aligned language models compromises safety, even when users do not intend to! In
609 *International Conference on Learning Representations*, 2024.
- 610 Rafael Rafailov, Archit Sharma, Eric Mitchell, Christopher D Manning, Stefano Ermon, and Chelsea
611 Finn. Direct preference optimization: Your language model is secretly a reward model. *Advances
612 in Neural Information Processing Systems*, 36, 2024.
613
- 614 Machel Reid, Nikolay Savinov, Denis Teplyashin, Dmitry Lepikhin, Timothy Lillicrap, Jean-baptiste
615 Alayrac, Radu Soricut, Angeliki Lazaridou, Orhan Firat, Julian Schrittwieser, et al. Gemini
616 1.5: Unlocking multimodal understanding across millions of tokens of context. *arXiv preprint
617 arXiv:2403.05530*, 2024.
- 618 Nisan Stiennon, Long Ouyang, Jeffrey Wu, Daniel Ziegler, Ryan Lowe, Chelsea Voss, Alec Radford,
619 Dario Amodei, and Paul F Christiano. Learning to summarize with human feedback. *Advances in
620 Neural Information Processing Systems*, 33:3008–3021, 2020.
621
- 622 Alessandro Stolfo, Yonatan Belinkov, and Mrinmaya Sachan. A mechanistic interpretation of
623 arithmetic reasoning in language models using causal mediation analysis. In Houda Bouamor, Juan
624 Pino, and Kalika Bali (eds.), *Proceedings of the 2023 Conference on Empirical Methods in Natural
625 Language Processing*, pp. 7035–7052, Singapore, December 2023. Association for Computational
626 Linguistics. doi: 10.18653/v1/2023.emnlp-main.435. URL [https://aclanthology.org/
627 2023.emnlp-main.435](https://aclanthology.org/2023.emnlp-main.435).
- 628 Gemma Team, Morgane Riviere, Shreya Pathak, Pier Giuseppe Sessa, Cassidy Hardin, Surya
629 Bhupatiraju, Léonard Hussenot, Thomas Mesnard, Bobak Shahriari, Alexandre Ramé, et al.
630 Gemma 2: Improving open language models at a practical size. *arXiv preprint arXiv:2408.00118*,
631 2024.
- 632 Hugo Touvron, Louis Martin, Kevin Stone, Peter Albert, Amjad Almahairi, Yasmine Babaei, Nikolay
633 Bashlykov, Soumya Batra, Prajjwal Bhargava, Shruti Bhosale, et al. Llama 2: Open foundation
634 and fine-tuned chat models. *arXiv preprint arXiv:2307.09288*, 2023.
635
- 636 Ashish Vaswani, Noam Shazeer, Niki Parmar, Jakob Uszkoreit, Llion Jones, Aidan N Gomez, Łukasz
637 Kaiser, and Illia Polosukhin. Attention is all you need. In *Advances in Neural Information
638 Processing Systems*, 2017.
639
- 640 Alexander Wei, Nika Haghtalab, and Jacob Steinhardt. Jailbroken: How does llm safety training fail?
641 *Advances in Neural Information Processing Systems*, 36, 2024.
- 642 Zheng-Xin Yong, Cristina Menghini, and Stephen H. Bach. Low-resource languages jailbreak gpt-4,
643 2024. URL <https://arxiv.org/abs/2310.02446>.
644
- 645 Longhui Yu, Weisen Jiang, Han Shi, YU Jincheng, Zhengying Liu, Yu Zhang, James Kwok, Zhenguo
646 Li, Adrian Weller, and Weiyang Liu. Metamath: Bootstrap your own mathematical questions for
647 large language models. In *The Twelfth International Conference on Learning Representations*,
2024.

648 Zheng Yuan, Hongyi Yuan, Chuanqi Tan, Wei Wang, Songfang Huang, and Fei Huang. Rrhf:
649 Rank responses to align language models with human feedback without tears. *arXiv preprint*
650 *arXiv:2304.05302*, 2023.

651 Yi Zeng, Hongpeng Lin, Jingwen Zhang, Diyi Yang, Ruoxi Jia, and Weiyang Shi. How johnny can
652 persuade llms to jailbreak them: Rethinking persuasion to challenge ai safety by humanizing llms.
653 *arXiv preprint arXiv:2401.06373*, 2024.

654 Wenxuan Zhang, Hou Pong Chan, Yiran Zhao, Mahani Aljunied, Jianyu Wang, Chaoqun Liu, Yue
655 Deng, Zhiqiang Hu, Weiwen Xu, Yew Ken Chia, et al. Seallms 3: Open foundation and chat
656 multilingual large language models for southeast asian languages. *arXiv preprint arXiv:2407.19672*,
657 2024.

658 Jiachen Zhao, Zhun Deng, David Madras, James Zou, and Mengye Ren. Learning and forgetting
659 unsafe examples in large language models. In *Forty-first International Conference on Machine*
660 *Learning*, 2024a.

661 Yiran Zhao, Wenxuan Zhang, Guizhen Chen, Kenji Kawaguchi, and Lidong Bing. How do large
662 language models handle multilingualism? *arXiv preprint arXiv:2402.18815*, 2024b.

663 Yiran Zhao, Wenxuan Zhang, Huiming Wang, Kenji Kawaguchi, and Lidong Bing. Adamergex:
664 Cross-lingual transfer with large language models via adaptive adapter merging. *arXiv preprint*
665 *arXiv:2402.18913*, 2024c.

666 Yiran Zhao, Wenyue Zheng, Tianle Cai, Xuan Long Do, Kenji Kawaguchi, Anirudh Goyal, and
667 Michael Shieh. Accelerating greedy coordinate gradient via probe sampling. *arXiv preprint*
668 *arXiv:2403.01251*, 2024d.

669 Chunting Zhou, Pengfei Liu, Puxin Xu, Srinivasan Iyer, Jiao Sun, Yuning Mao, Xuezhe Ma, Avia
670 Efrat, Ping Yu, Lili Yu, et al. Lima: Less is more for alignment. *Advances in Neural Information*
671 *Processing Systems*, 36, 2024.

672 Andy Zou, Zifan Wang, Nicholas Carlini, Milad Nasr, J Zico Kolter, and Matt Fredrikson. Universal
673 and transferable adversarial attacks on aligned language models. *arXiv preprint arXiv:2307.15043*,
674 2023.

675 Andy Zou, Long Phan, Justin Wang, Derek Duenas, Maxwell Lin, Maksym Andriushchenko, Rowan
676 Wang, Zico Kolter, Matt Fredrikson, and Dan Hendrycks. Improving alignment and robustness
677 with circuit breakers, 2024.

681 A APPENDIX

682 A.1 PARALLEL NEURON DETECTION METHOD

683 **Feed-Forward Network (FFN)** In the latest open-source models, when processing input c , the
684 feed-forward network in a certain layer is defined as

$$685 \text{FFN}(x) = \left(\text{SiLU}(W_{\text{gate}}(x)) \cdot W_{\text{up}}(x) \right) W_{\text{down}}, \quad (7)$$

686 where $x \in \mathbb{R}^{l \times d_{\text{model}}}$ is the embedding fed into the FFN, $W_{\text{gate}}, W_{\text{up}} \in \mathbb{R}^{d_{\text{model}} \times d_{\text{inter}}^2}$, $W_{\text{down}} \in$
687 $\mathbb{R}^{d_{\text{inter}} \times d_{\text{model}}}$. The calculation of the importance of the k -th neuron in W_{up} , when processing the
688 input c , as presented in Equation 2, can be equivalently transformed to

$$689 \text{Imp}(W_{\text{up}}[:, k] | c) = \|\widehat{\text{FFN}}(x) - \text{FFN}(x)\|_2 = \left\| (h_{\text{ffn}}(x) \cdot \text{Mask}[k]) W_{\text{down}} \right\|_2, \quad (8)$$

690 where $h_{\text{ffn}} \in \mathbb{R}^{l \times d_{\text{inter}}}$ represents the embedding before W_{down} , and $\text{Mask}[k] \in d_{\text{inter}}$ is a vector
691 with the k -th element equal to 1 and the rest equal to 0. To calculate $\text{Imp}(W_{\text{up}}[:, k] | c)$ for $k \in d_{\text{inter}}$
692 parallelly, we introduce a diagonal mask matrix of size $(d_{\text{inter}}, d_{\text{inter}})$, denoted as Mask . Therefore,

$$693 \text{Imp}(W_{\text{up}} | c) = \|(h_{\text{ffn}}(x) \cdot \text{Mask}) W_{\text{down}}\|_2. \quad (9)$$

694 Furthermore, we observe that deactivating the k -th neuron of W_{down} is equivalent to deactivating the
695 k -th neuron in W_{up} , as they both result in $h_{\text{ffn}}[k] = 0$. Hence, we can also derive $\text{Imp}(W_{\text{down}} | c)$ by
696 employing Equation (9).

700 ² $W(\cdot)$ represents the linear matrix product of the input x and the parameter W , i.e., $W(x) := xW$.

Self-Attention Network When processing input c , the self-attention network in a certain layer is

$$\text{Attention}(x) = \text{Softmax}\left(\frac{W_Q(x)W_K^T(x)}{\sqrt{d}}\right)W_V(x), \quad (10)$$

where $W_Q, W_K, W_V \in \mathbb{R}^{d_{model} \times d_{mid}}$.³ Since $W_V(x)$ is not in the non-linear softmax calculation, we can calculate $\text{Imp}(W_V|c)$ by applying Equation (9). For W_Q , we obtain $\text{Imp}(W_Q[:, k]|c)$ by deactivating its k -th neuron, specifically, $\hat{W}_Q \leftarrow W_Q[:, k] = 0$. Firstly, we calculate the difference in attention weight before and after deactivation, prior to scaling and softmax,

$$\Delta_k(x) = \hat{W}_Q(x)W_K^T(x) - W_Q(x)W_K^T(x) = W_Q(x)[:, k]W_K(x)[k, :] \in \mathbb{R}^{l \times l}. \quad (11)$$

Next, as the changes in attention exhibit a positive correlation with the changes in the output of this layer, the importance of $W_Q[:, k]$ in processing c , can be approximated as

$$\begin{aligned} \text{Imp}(W_Q[:, k]|c) &\approx \|\text{attention}(x) - \text{attention}(x)\|_2 \\ &\approx \left\| \text{softmax}\left(\frac{W_Q(x)W_K^T(x) - \Delta_k(x)}{\sqrt{d}}\right) - \text{softmax}\left(\frac{W_Q(x)W_K^T(x)}{\sqrt{d}}\right) \right\|_2. \end{aligned} \quad (12)$$

This process can also be calculated in parallel, specifically,

$$\begin{aligned} \Delta(x) &= \hat{W}_Q(x)W_K^T(x) - W_Q(x)W_K^T(x) \\ &= W_Q(x).\text{resize}(l, 1, d_{mid}) \times W_K(x).\text{resize}(1, l, d_{mid}) \in \mathbb{R}^{l \times l \times d_{mid}}. \end{aligned} \quad (13)$$

Therefore, the importance of W_Q in processing input c is calculated by

$$\text{Imp}(W_Q|c) \approx \left\| \text{softmax}\left(\frac{W_Q(x)W_K^T(x) - \Delta(x)}{\sqrt{d}}\right) - \text{softmax}\left(\frac{W_Q(x)W_K^T(x)}{\sqrt{d}}\right) \right\|_2. \quad (14)$$

Similarly, since W_K is symmetrical to W_Q , $\text{Imp}(W_K|c)$ can be calculated in the same way.

A.2 SAFETY NEURON DETECTION CORPUS

In the neuron detection process, we utilize the training documents from Zou et al. (2024), from which sampling 200 documents for detection. Specifically, the training set contains harmful queries across various categories, including “terrorism and violent extremism”, “self-harm”, and “political campaigning”, etc. This diverse dataset helps ensure the generalizability of the detected neurons. Furthermore, our analysis examined how the number of input documents affects safety neuron detection, as shown in Table 5. The ablation analysis is on Llama3-8B-Instruct, and the results demonstrate that 200 documents are sufficient to reliably identify safety neurons.

Table 5: Number of detected safety neurons across different document sizes.

Corpus Size	10	50	100	200	400	800
Number of Safety Neurons	8912	4825	3594	2329	2322	2314

³In some models like Vicuna and Mistral, $d_{model} = d_{mid}$, but we use different notations to avoid ambiguity.